

D-galactose protects the intestine from ionizing radiation-induced injury by altering the gut microbiome

Tong Zhu¹, Zhouxuan Wang¹, Junbo He^{1,2}, Xueying Zhang¹,
Changchun Zhu¹, Shuqin Zhang¹, Yuan Li¹ and Saijun Fan^{1,*}

¹Tianjin Key Laboratory of Radiation Medicine and Molecular Nuclear Medicine, Department of Radiation Injury Treatment, Institute of Radiation Medicine Chinese Academy of Medical Sciences and Peking Union Medical College, 238 Baidi Road, Tianjin 300192, China

²Department of Radiation Oncology, Fudan University Shanghai Cancer Center, 270 Dong' An Road, Shanghai 200032, PR China

*Corresponding author. Saijun Fan, Institute of Radiation Medicine Chinese Academy of Medical Sciences and Peking Union Medical College.
Email: fansaijun@irm-cams.ac.cn.

Tong Zhu and Zhouxuan Wang contributed equally to this work.

(Received 24 February 2022; revised 18 May 2022; editorial decision 19 August 2022)

ABSTRACT

This article aims to investigate the protection of the intestine from ionizing radiation-induced injury by using D-galactose (D-gal) to alter the gut microbiome. In addition, this observation opens up further lines of research to further increase therapeutic potentials. Male C57BL/6 mice were exposed to 7.5 Gy of total body irradiation (TBI) or 13 Gy of total abdominal irradiation (TAI) in this study. After adjustment, D-gal was intraperitoneally injected into mice at a dose of 750 mg/kg/day. Survival rates, body weights, histological experiments and the level of the inflammatory factor IL-1 β were observed after TBI to investigate radiation injury in mice. Feces were collected from mice for 16S high-throughput sequencing after TAI. Furthermore, fecal microorganism transplantation (FMT) was performed to confirm the effect of D-gal on radiation injury recovery. Intraperitoneally administered D-gal significantly increased the survival of irradiated mice by altering the gut microbiota structure. Furthermore, the fecal microbiota transplanted from D-gal-treated mice protected against radiation injury and improved the survival rate of recipient mice. Taken together, D-gal accelerates gut recovery following radiation injury by promoting the growth of specific microorganisms, especially those in the class *Erysipelotrichia*. The study discovered that D-gal-induced changes in the microbiota protect against radiation-induced intestinal injury. *Erysipelotrichia* and its metabolites are a promising therapeutic option for post-radiation intestinal regeneration.

Keywords: Radiation injury; gut microbiota; fecal microbiota transplantation; D-galactose (D-gal)

INTRODUCTION

The widespread use of ionizing radiation for cancer treatment is associated with side effects that lower the quality of life of patients [1, 2]. Radiation injury primarily affects the hematopoietic, gastrointestinal (GI) and nervous systems [3–5] and depends on the dose of radiation. Radiation-induced GI injury usually manifests as dyspepsia, nausea, vomiting and diarrhea and can even be life-threatening [6, 7]. Several research groups have identified small-molecule compounds that effectively mitigate radiation toxicity in the gut [8–11]. Furthermore, the intestinal flora is also intimately involved in mediating radiation-induced GI toxicity.

The gut microbiota comprises bacteria, viruses and fungi and its structure and diversity are affected by multiple factors, such as diet,

medication and environmental stimuli [12]. The dominant phyla in the human intestine are *Actinobacteria*, *Bacteroidetes*, *Fusobacteria*, *Firmicutes* and *Proteobacteria* [13]. Studies show that radiotherapy induces gut dysbiosis, and the composition of the gut microbiota of irradiated patients is significantly different from that of non-irradiated patients and healthy control subjects. *Fusobacteria*, *Euryarchaeota* and *Tenericutes* are abundant in the intestines of patients with cancer [14, 15]. Radiotherapy significantly increases the abundance of *Actinobacteria* and *Firmicutes* and decreases that of *Bacteroidetes*, *Fusobacteria* and *Proteobacteria*. An increased *Firmicutes* diversity and a higher *Firmicute/Bacteroidetes* ratio in the small intestine are characteristics of GI mucositis [16, 17]. Consistent with this finding, the higher proportion of *Firmicutes* induced by radiotherapy is the factor causing radiation-

induced diarrhea. On the other hand, several gut microorganisms are known to promote intestinal regeneration following radiation damage. For instance, lactic acid-producing bacteria such as *Bifidobacterium* and *Lactobacillus plantarum* promote intestinal stem cell (ISC) proliferation in damaged tissues by producing lactic acid that activates the G-protein coupled receptor Gpr81 via the Wnt/ β -catenin signaling pathway [18].

D-galactose (D-gal) has been widely used to induce aging models in some antiaging pharmacological studies. As reported in previous studies, after 45 days of subcutaneous injection, the levels of malondialdehyde (MDA) and reactive oxygen species (ROS) increased in many organs of mice, such as the brain, blood and liver [19, 20]. According to the oxidative stress induced by D-gal, subcutaneous or intraperitoneal injection treatment for over 6 weeks in mice usually induces brain aging and related mechanisms, including recognition and spatial memory impairments [21–23]. However, the effect of D-gal on radiation damage recovery is unknown.

In this study, we found that intraperitoneal administration of D-gal increased the survival rate and body weight of irradiated mice by protecting GI tract injury. D-gal altered the gut microbiota, and fecal microorganism transplantation (FMT) from D-gal-treated mice significantly protected against radiation-induced GI injury in recipients. Our findings provide a solid basis for employing the gut microbiota and microbial metabolites as treatments for GI injury.

MATERIALS AND METHODS

Mouse irradiation and treatment regimen

Six- to 8-week-old male C57BL/6 J mice were purchased from HFK Bioscience (Beijing, China) and housed in the Institute of Radiation Medicine (IRM) of Chinese Academy of Medical Sciences (CAMS) at $22 \pm 2^\circ\text{C}$ and 40–70% humidity on a 12 h/12 h light/dark cycle. The study was performed in compliance with the ARRIVE guidelines. All *in vivo* studies were approved by the Institutional Animal Care and Use Committee of IRM-CAMS under Permit No. IRM-DWLL-2021092.

Starting seven days before irradiation, the mice were injected intraperitoneally with D-gal (Sango Biotech, Shanghai, China) in saline at a dose of 15 mg daily (as shown in Fig. 1A) for both the total body irradiation (TBI) and total abdominal irradiation (TAI) strategies. For TBI, the mice were exposed to a total dose of 7.5 Gy of ^{137}Cs gamma rays using a Gammacell 40 Exactor (0.84 Gy/min, Atomic Energy of Canada Lim, Chalk Rive, Canada). For TAI, mice were anesthetized and exposed to a total dose of 13 Gy in a specific shielding facility. The shielding tray was made by lead block with 6 holes of 3 cm diameter. The abdomen of a mouse was placed to the location of the hole and ensure other parts of body are in the shielded area. The irradiated mice were housed in individual cages and injected daily with D-gal for 7 days. For the observation of survival rates and body weights, mice were irradiated using the TBI strategy. Data were collected until the thirtieth day after irradiation. For further investigation of radiation-induced intestinal injury, mice were euthanized on the seventh day after TBI, and the colons and small intestines were excised, measured or frozen for subsequent assays. Some animals died before collection due to radiation injury. Dead animals were disposed according to rules in the institute. Data from histology and real-time polymerase chain reaction (PCR) analyses did not include dead animals.

Fecal DNA isolation and sequencing

Twelve mice in each group were analyzed and were divided into two cages for maintenance. Mice in each group were mixed and re-separated in cages every 2 days to exclude the effect of the environment and hierarchy building on the microbiota. Mice from the same group were regarded as biological replicates, but not due to any other standards, like cages. Stool samples were collected on Days 0, 5 and 10 after irradiation and stored at -80°C . For collection on Day 0, feces were collected 4 hours after treatment with D-gal. After fecal collection on Day 0, the mice were exposed to irradiation.

The 16S rRNA V4 region was amplified with 515F and 806R primers (0.2 μM each) using 15 μl of Phusion[®] High-Fidelity PCR Master Mix (New England Biolabs) and ~ 10 ng of the DNA template. The thermal cycling parameters were as follows: initial denaturation at 98°C for 1 min, followed by 30 cycles of denaturation at 98°C for 10 s, annealing at 50°C for 30 s and elongation at 72°C for 30 s and a final elongation at 72°C for 5 min. Sequencing libraries were generated using a TruSeq[®] DNA PCR-Free Sample Preparation Kit (Illumina, USA) according to the manufacturer's instructions, and index codes were added. The quality of the library was assessed using a Qubit[®] 2.0 Fluorometer (Thermo Scientific) and Agilent Bioanalyzer 2100 system and sequenced with the Illumina NovaSeq platform to generate 250 bp paired-end reads.

Fecal microorganism transplantation

Twelve 6- to 8-week-old male C57BL/6 mice in the recipient group were housed in two cages. To normalize the microbiota in each group, Mice were mixed and re-separated every 2 days to normalize the microbiota in each group. Before FMT, recipient mice were treated with antibiotics (1000 $\mu\text{g}/\text{ml}$ ampicillin and 500 $\mu\text{g}/\text{ml}$ streptomycin) in drinking water for 4 weeks.

Donor mice were injected intraperitoneally with 750 mg/kg D-gal or saline daily for 7 days. Twelve mice were included in each donor group. Mice were mixed and separated as described in section 2.2 to normalize the microbiota in each group. Two pieces of feces were collected from each donor mouse daily. All the feces from one group were mixed and weighed. Feces were diluted in saline with 1 ml per 0.1 g. Further experiments were performed as described by Ming Cui *et al.* [24]. The supernatant of the fecal mixture was administered to mice in the FMT group by oral gavage.

Enzyme-linked immunosorbent assay (ELISA)

Frozen tissue samples were weighed and homogenized in chilled Phosphate Buffered Saline (PBS). After reconstituting to 0.1 g/ml, the homogenates were centrifuged at 12000 rpm for 10 min at 4°C . The supernatants were collected and analyzed using an ELISA kit (MIBio, China) according to the manufacturer's instructions. Absorbance values at 450 nm were measured with a spectrophotometer (Rayto, China). The relevant concentration of total protein were measured using BCA protein detection kit (Solarbio, China).

Polymerase chain reaction

The frozen colon samples were subjected to Ribonucleic Acid (RNA) extraction, reverse transcription, Reversed Transcript Polymerase

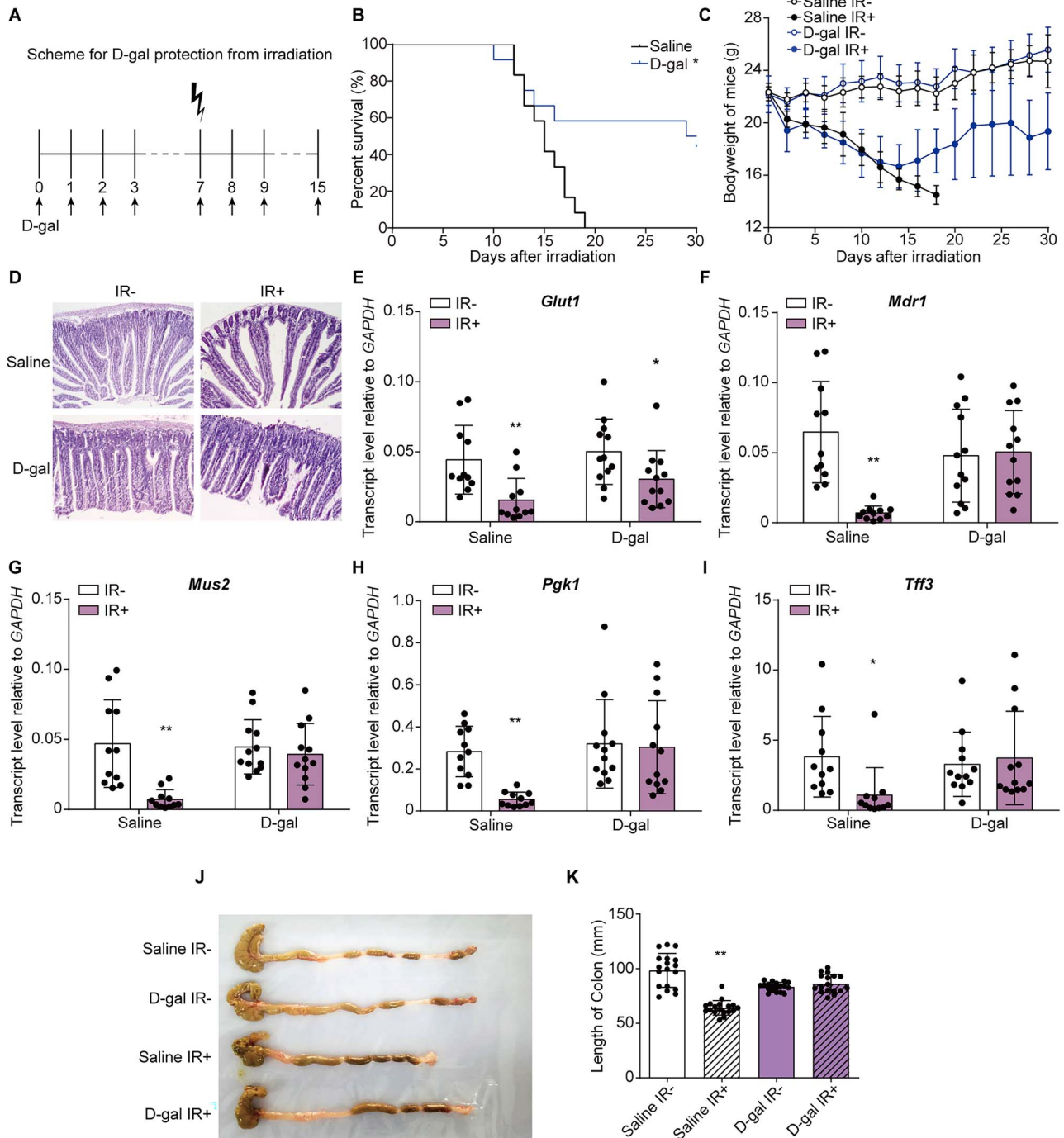


Fig. 1. D-gal injection increased the survival rate of irradiated mice and restored the structure of the mouse small intestine. (A) Experimental outline of irradiation and D-gal administration. D-gal was injected starting 7 days before irradiation and 7 days after TBI. (B-C) Kaplan–Meier survival curve (B) and body weights (C) of mice in the saline- and D-gal-treated groups after 7.5 Gy of TBI; There are 36 mice in each group. $P = 0.0137$ in (B). The significance analysis were obtained from Graphpad analysis by Log-rank (Mantel-Cox) test. (D) Representative images of =H&E-stained small intestine sections from the indicated groups. (E–I) The transcript levels of *Glut1* (E), *Mdr1* (F), *Mus2* (G), *Pkg1* (H) and *Tff3* (I) in the small intestine of mice exposed to the indicated treatments. The error bars in graphs means standard deviation of indicated data. * $P < 0.05$, ** $P < 0.01$; $n = 12$ animals per group. Data were analyzed for differences using independent samples t-test. Stars without a horizontal line were generated by comparing the IR-group in indicated treatment. Stars with a horizontal line mean that the two groups were compared. (J) Representative images

Chain Reaction (RT-PCR) and Quantitative Real-time Polymerase Chain Reaction (qRT-PCR) as described by Ming Cui *et al.* [25]. Primer sequences are listed in [Supplementary Table S1](#).

Western blotting

The tissues were lysed with RIPA buffer (Solarbio, China) on ice and centrifuged at 12000 g for 15 min at 4°C. The proteins in the supernatant were separated on 12% SDS-PAGE gels and transferred to polyvinylidene fluoride (PVDF) membranes. After blocking with 5% skim milk, the membranes were probed with an anti-p16 primary antibody (Abcam #ab51243, Cambridge, USA), followed by Fluorescein Isothiocyanate (FITC)-conjugated goat anti-rabbit IgG (H + L) (Proteintech Group, USA).

Cell culture

The human enterocyte HIEC-6 cell line (purchased from ATCC, CRL-3266) was cultured in RPMI-1640 medium (Gibco, CA) supplemented with 10% fetal bovine serum (Gibco, CA) at 37°C with 5% CO₂. The cells were treated with 0.008 g/ml D-gal or water for 24 h and then irradiated with a single dose of 4 Gy.

Transcriptome analysis

RNA was extracted from HIEC-6 cells receiving the indicated treatments using TRIzol, and 3 µg of RNA per sample were used for the transcriptome analysis. Sequencing libraries were generated using the NEBNext® Ultra™ RNA Library Prep Kit for Illumina® (NEB, USA) according to the manufacturer's instructions, and index codes were added to attribute sequences to each sample. The indexed samples were clustered with a cBot Cluster Generation System using TruSeq PE Cluster Kit v3-cBot-HS (Illumina) according to the manufacturer's instructions. The library was then sequenced using the Illumina HiSeq platform, and 125 bp/150 bp paired-end reads were generated.

Histology assays

Mice in each group were euthanized on the fifteenth day after TAI, and the small intestines were excised. Samples were fixed overnight with 4% paraformaldehyde and gradually dehydrated with a gradient of ethanol solutions. Then, tissues were embedded in paraffin and sectioned. For hematoxylin and eosin (H&E) staining, sections were stained with hematoxylin (Solarbio, #H8070) and eosin (Solarbio, G1100). For immunohistochemistry, the primary antibody against *Lgr5* was purchased from Abcam (#ab273092). For immunofluorescence staining, the primary antibody against Ki67 was purchased from Cell Signaling Technology (#12075). To quantify the damage in the small intestine, the length of villi and the fluorescence intensity of *Lgr5* and Ki67 staining were measured using ImageJ software.

Statistical analysis

Each experiment was repeated at least three times. Two groups of a single variable were compared using independent samples t-test. The survival results of mice were assessed using Log-rank (Mantel-Cox)

test. The 16S rRNA sequencing results were assessed using Tukey's honestly significant difference (HSD) test, and two-way ANOVA was used to compare body weights. $P < 0.05$ was considered statistically significant. The error bars marked in the graphs all indicate the standard deviation of the data.

RESULTS

D-galactose protected against radiation-induced GI injury in mice

D-gal was first used to induce aging in our project by administering it at a dose of 400 mg/kg/day for 30 days [26]. After exposure to gamma radiation, we surprisingly observed significantly increased survival of mice ([Supplementary Fig. 1A](#)). The body weights of the mice recovered after 15 days ([Supplementary Fig. 1B](#)). However, after administering 500 mg/kg/day D-gal by oral gavage for 4 weeks [27], we investigated the survival of mice administered 7.5 Gy of TBI. Survival was not significantly altered ([Supplementary Fig. 1C](#)). These results suggested that oral gavage of D-gal does not change the survival rates of mice. According to research on pancreatic dysfunction induced by D-gal, we tried to shorten the duration of D-gal injection. However, D-gal injection at 400 mg/kg/day was not effective for short-term treatment ([Supplementary Fig. 1D](#)). Since the effective concentration of D-gal ranged from 100 mg/kg [28] to 1000 mg/kg [29] in previous studies, we adjusted the concentration to 750 mg/kg/day and achieved 50% survival ([Supplementary Fig. 1E–F](#)). Thus, the protective effect of D-gal on radiation injury is a dose dependent issue. After performing the preliminary experiments at 24 h, 2 d, or 4 d before irradiation ([Supplementary Fig. 1G](#)), the optimal time was 7 days.

The mice were intraperitoneally injected with 750 mg/kg/day D-gal and irradiated as described in the methods ([Fig. 1A](#)). D-gal injection increased the survival rates of mice by 50% and restored their body weights on the fifteenth day after the administration of 7.5 Gy of TBI ([Fig. 1B–C](#)). Furthermore, D-gal also alleviated structural damage to the small intestine ([Fig. 1D](#)). The villus length in the D-gal injection group was maintained compared to that in the 'Saline IR-' group after irradiation ([Supplementary Fig. 2A](#)). Consistent with this finding, the relative expression levels of genes involved in maintaining epithelial integrity, including *Glut1*, *Mdr1*, *Mus2*, *Pgk1* and *Tff3*, were significantly decreased after irradiation. D-gal-treatment maintained the mRNA expression of these genes after irradiation ([Fig. 1E–I](#)). As shown in [Fig. 1J–K](#), the colons of the D-gal group were also longer than those of saline controls after TBI. We analyzed the *in situ* expression of the ISC markers *Lgr5* and Ki67 in proliferating cells to further confirm the post-irradiation recovery of the small intestine following D-gal treatment. As shown in [Fig. 2A–B](#), D-gal significantly increased the expression of *Lgr5* in intestinal crypt cells after irradiation. The area fraction of Ki67⁺ cells was significantly increased after D-gal injection and irradiation ([Fig. 2C–D](#)), indicating increased proliferation and renewal. Finally, the level of the inflammatory factor IL-1β in the small intestine was not increased after D-gal treatment and irradiation, which also indicated tissue recovery and regeneration ([Fig. 2E](#)).

of colons extracted from mice exposed to the indicated treatments on Day 15 after TBI. (K) The length of colons in the indicated groups. The error bars in graphs means standard deviation of indicated data. ** $P < 0.01$; $n = 12$ mice per group. Data were analyzed for differences using independent samples t-test. Stars without a horizontal line were generated by comparing the 'Saline IR-' group.

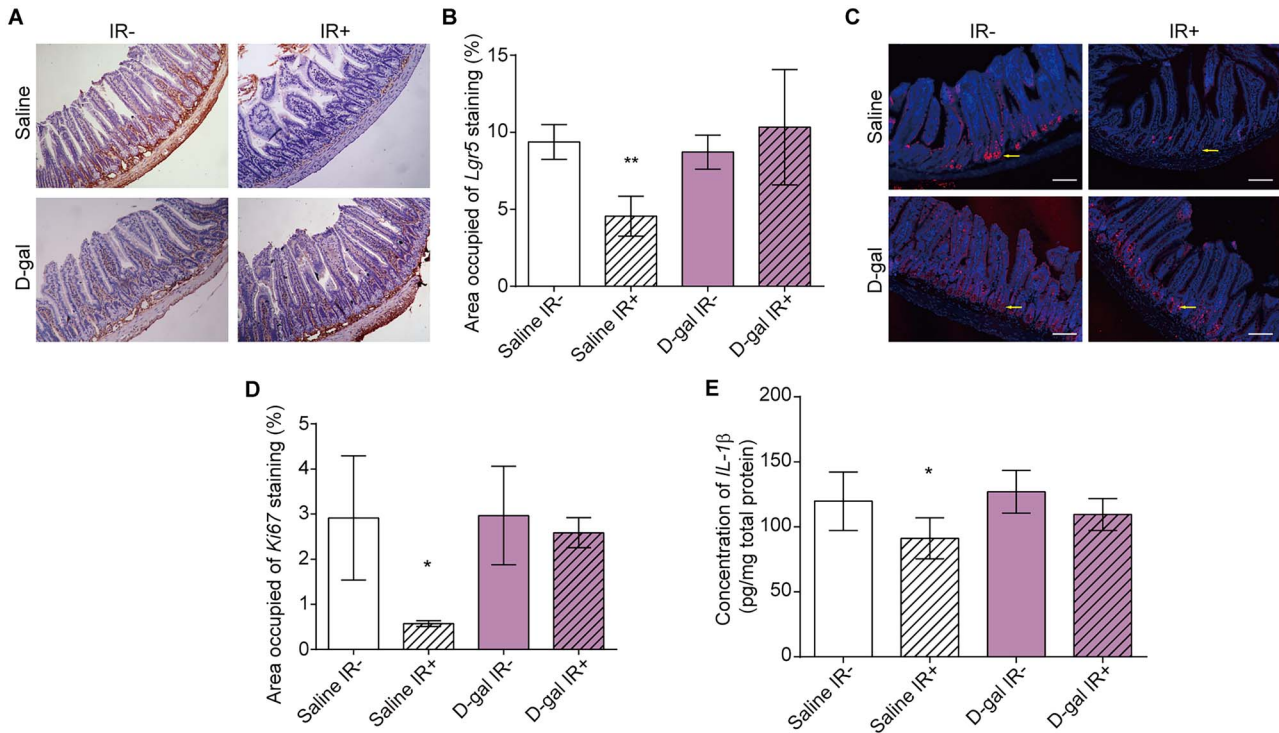


Fig. 2. D-gal injection alleviated radiation-induced small intestinal injury in mice. (A) Representative images of immunohistochemical staining showing the *in situ* expression of *Lgr5* in the intestinal crypts of mice exposed to the indicated treatments. Small intestines were collected on the fifteenth day after the administration of 7.5 Gy of TBI and stained with H&E. (B) Statistical analysis of *Lgr5*-positive cells in immunohistochemistry assays. Data were collected from more than six images in the same field of view. The area fraction of *Lgr5*+ cells was analyzed using ImageJ software. The error bars in graphs means standard deviation of indicated data. (C) Representative images of immunofluorescence staining showing *Ki67*-positive cells in the small intestine of the indicated groups (red, *Ki67*; blue, DAPI). Yellow arrows indicate the location of *Ki67*. The small intestines were collected on the fifteenth day after irradiation in each group. The images were scanned and captured using a laser confocal microscope (Leica). (D) Statistical analysis of *Ki67*-positive cells in each group. Data were collected from more than six images in the same field of view. The data were analyzed using ImageJ software. The error bars in graphs means standard deviation of indicated data. (E) IL-1 β levels in intestinal homogenates measured using ELISA. Small intestines were collected on the 15th day after the administration of 7.5 Gy of TBI. The procedure was performed according to the instructions provided with the ELISA kit. Data were analyzed using a microplate reader. The error bars in graphs means standard deviation of indicated data. ** $P < 0.01$; n.s., not significant; $n = 12$ mice per group. Data in (B), (D) and (E) were analyzed for differences using independent samples t-test. Stars without a horizontal line were generated by comparing the ‘Saline IR-’ group. Stars with a horizontal line mean that the two groups were compared.

D-gal altered the gut microbiota composition

Since D-gal alleviates radiation-induced small intestine injury, we used the radiation intestinal injury mouse model for further experiments to avoid the crosstalk between other organs and gut microbiota [30–32]. Mice were irradiated with 13 Gy of TAI. To confirm the protective effect of D-gal in TAI radiation protocol, we observed the survival of mice after TAI with or without D-gal treatment (Fig. S1H). D-gal elevated the survival rate of mice after TAI. The fecal microbiota is a determining factor of post-irradiation recovery and survival [24]. Therefore, we analyzed the fecal microbiota composition of the differentially treated mice by performing 16S high-throughput sequencing. Fig. 3A–C shows the results of alpha diversity of microbiota, which represents the species richness. As shown in Fig. 3A–C, the observed species between D-gal- and saline-treated mice were not significantly altered over time after irradiation. On the other hand, the alpha

diversity of microbiota in D-gal- and Saline-treated mice without irradiation was shown in supplementary data (Supplementary Fig. 3A). D-gal injection did not change the amount of species in feces both in non-irradiation and irradiation group. However, D-gal treatment significantly altered beta diversity, which indicates the abundance of the colony. They were indicated by Principal Component Analysis (PCA) and Principal Co-ordinates Analysis (PCoA) on Days 0, 5 and 10 post-irradiation in Fig. 3D–I. Figure 3D–G shows the beta diversity determined using PCA and PCoA on Day 0 between D-gal and saline treatment groups. The significance is displayed as the P value shown in the PCoA plot (Fig. 3G). In addition, the significant change induced by D-gal treatment was maintained over time. The beta diversity measured on Day 5 (Fig. 3E–H) and Day 10 (Fig. 3F–I) also exhibited significant differences compared to saline treatment. However, the D-gal did not significantly change the beta diversity in non-irradiation

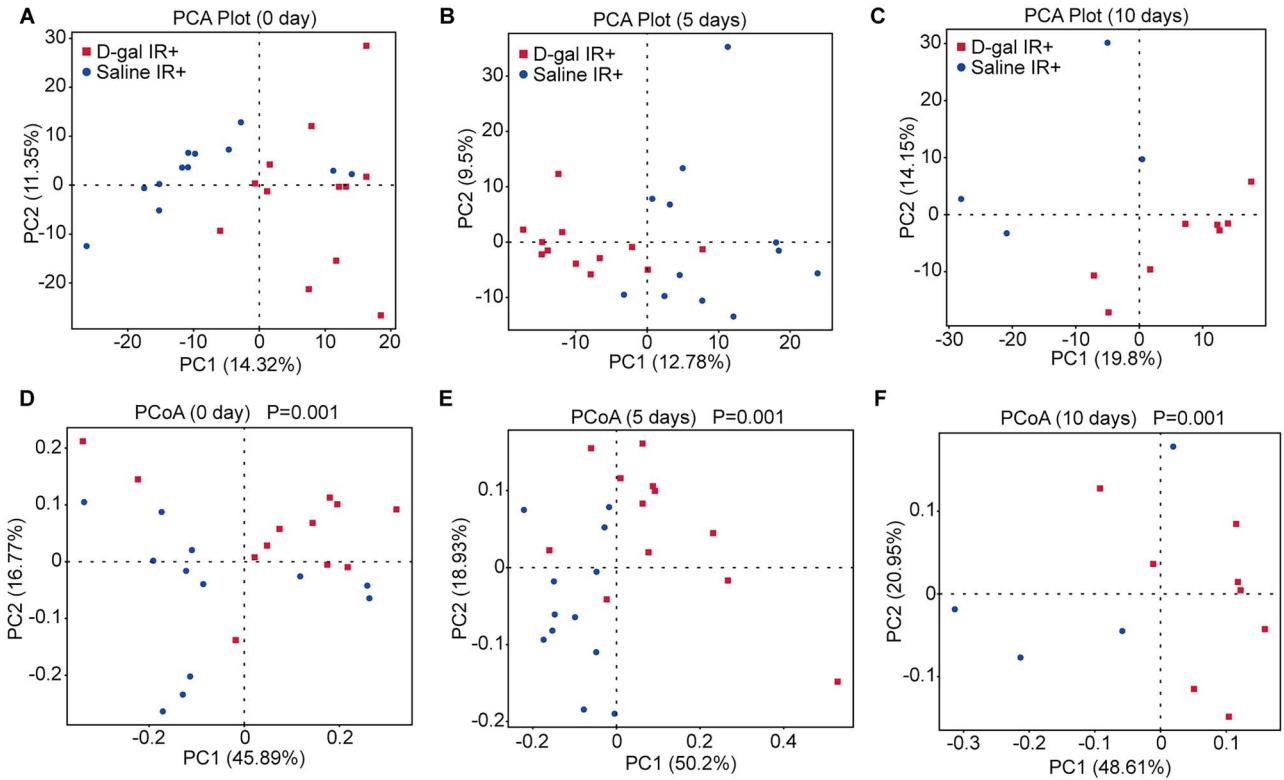


Fig. 3. D-gal injection influenced the microorganism structure of the gut microbiota in irradiated mice. (A–C) PCA analysis of the gut microbiota in mice from the ‘saline IR+’ and ‘D-gal IR+’ groups on Day 0 (A), Day 5 (B) and Day 10 (C) post-irradiation; $n \geq 10$ mice per group. (D–F) PCoA analysis of the gut microbiota in mice from the ‘saline IR+’ and ‘D-gal IR+’ groups on Day 0 (D), Day 5 (E) and Day 10 (F) post-irradiation; $n \geq 10$ mice per group. The difference in beta diversity was indicated by PERMANOVA and is shown as the P value in the PCoA plot.

group (Supplementary Fig. 3B–C). Thus, the microbiota structure was altered by D-gal supplementation after irradiation. Taken together, D-gal alters the structure of the gut microbiota and promotes the development of a novel microbial community in the radiation-exposed intestine. Based on the findings described thus far, the altered gut microbiome may play a pivotal role in protecting the intestine from ionizing radiation.

D-gal enriched specific microorganisms in the intestinal niche

We analyzed the intestinal microflora in saline- and D-gal-treated mice at the genus level to examine the hypothesis described above. We firstly summarized the effect of ionizing radiation on the beta-diversity of mouse intestinal flora without the influence of D-gal (Fig. 4A–B). The structure of the intestinal flora was significantly altered by ionizing radiation. Organisms belong to *Firmicutes* were significantly decreased as shown in Fig. 4A, meanwhile *Bacteroidetes* were increased. The enriched organisms in irradiated mice mostly belong to *Bacteroidetes* (Fig. 4B). As a comparison, D-gal-treatment could instead increase the enrichment of *Firmicutes* (Fig. 4C–D). As shown in Fig. 4C, the intestinal abundance of *Lactobacillus* (belongs to the class *Bacilli* of the phylum *Firmicutes*) was significantly decreased in the D-gal-injected mice ten days in the non-irradiation group compared to the

controls (Fig. 4C). In contrast, *Erysipelatoclostridium* were the most significantly affected genera in the D-gal-treated mice. As indicated by the LEfSe analysis (Fig. 4D), three significantly altered *Erysipelotrichia* microorganisms were detected in the D-gal non-irradiated group, whereas two microorganisms enriched in Saline non-irradiated group. The significantly enriched microorganisms in the D-gal-irradiated group belonged to the class *Bacilli* of the phylum *Firmicutes* as compared to Saline-irradiated group (Fig. 4E). In the irradiated D-gal group (Fig. 4F), the significantly predominant microorganisms in the phylum changed to *Clostridia*, *Clostridiales* and *Ruminococcaceae* and all belonged to the phylum *Firmicutes*. In contrast, only one *Firmicutes*-associated *Lactobacillus* species were observed in Saline-irradiated group. The predominant phylum detected after irradiation in the D-gal group was *Firmicutes*, and the class *Erysipelotrichia* was most abundant. Taken together, D-gal induces specific changes in the gut microbiome after irradiation, which might be beneficial for intestinal recovery from injury.

FMT from D-gal-treated mice protected radiation-induced GI injury

We transplanted the feces of D-gal-treated mice to recipients subjected to 7.5 Gy of TBI to further assess the role of the gut microbiota in radiation-induced GI injury (Fig. 5A). We collected feces from donor

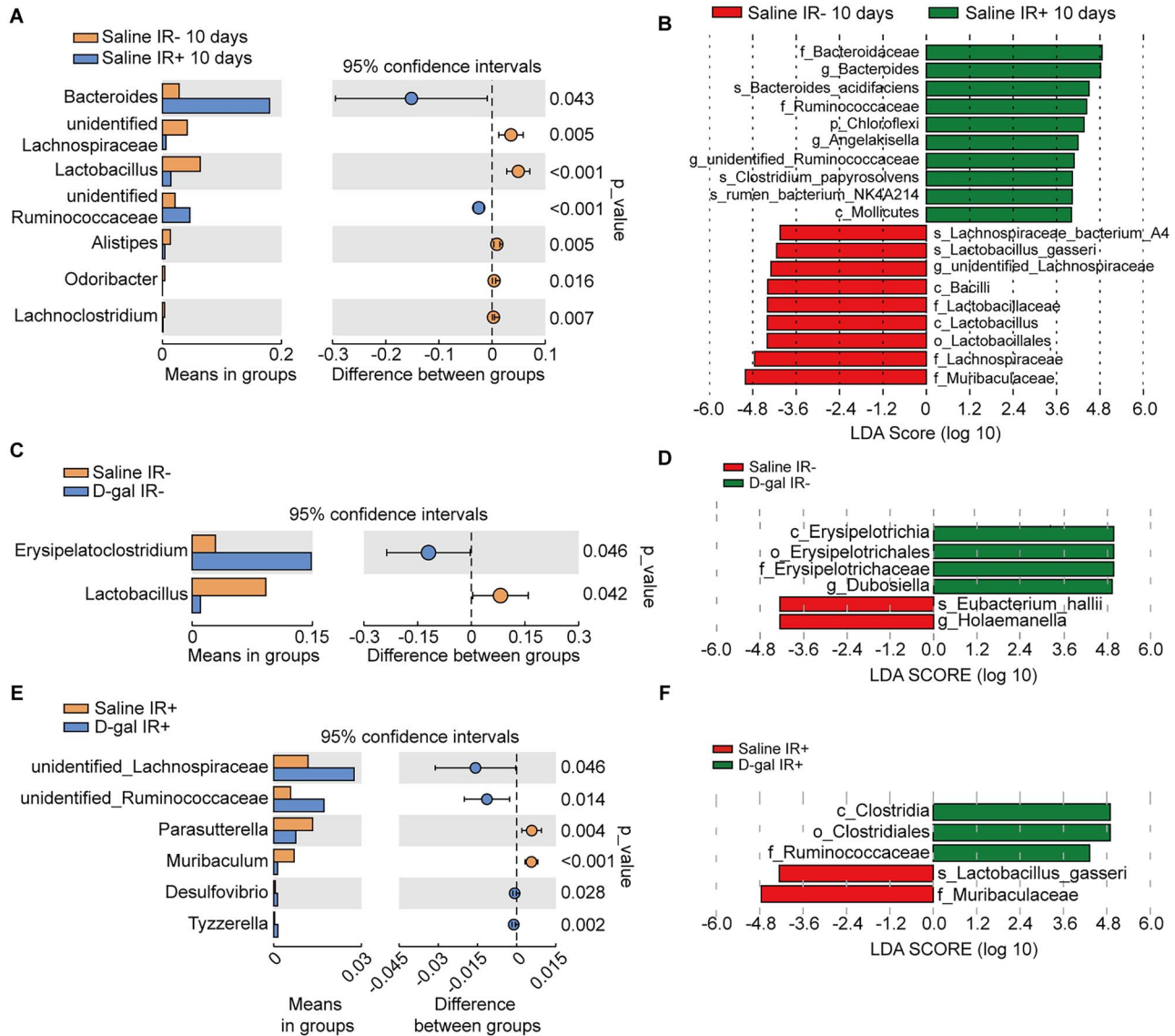


Fig. 4. D-gal altered the dominant bacteria in the intestinal microbiome. (A) Intestinal flora composition at genus level 10 days post-irradiation in ‘Saline IR-’ and ‘Saline IR+’ groups. (B) Linear discriminant analysis effect size (LEfSe) of gut microbiota in the saline group before and after 13Gy TAI. (C) Intestinal flora composition at the genus level measured at 10 days post-irradiation in the ‘Saline IR-’ and ‘D-gal IR-’ groups. (D) LEfSe of gut microbiota in the ‘Saline IR-’ and ‘D-gal IR-’ groups before and after the administration of 13 Gy of TAI. (E) Intestinal flora composition at the genus level measured at 10 days post-irradiation in the ‘Saline IR+’ and ‘D-gal IR+’ groups. (F) LEfSe of the gut microbiota in the aforementioned groups.

mice and recipient mice on the day before FMT and on the fifth day after FMT to ensure the efficiency of FMT. After treated with antibiotics for 4 weeks, the gut microbiota from recipient mice were totally different from donor mice before FMT (Supplementary Fig. 4A–F). The microbiota from donor mice treated with saline and D-gal was successfully established in the corresponding recipients after FMT for 5 days (Supplementary Fig. 4G–L). As shown in Fig. 5B, FMT from D-gal mice significantly increased the survival rates of the irradiated mice and restored their body weight to normal (Fig. 5C). The proportion of surviving mice transplanted with the feces from saline-treated mice

was significantly lower (Fig. 5B), and their body weight decreased steadily until the thirtieth day after irradiation before returning to normal (Fig. 5C). Thus, FMT from D-gal-treated mice accelerated recovery after TBI. Furthermore, we repeated the FMT assay and collected the small intestines from mice on the fifteenth day after the administration of 13 Gy of TAI to investigate abdominal injury in mice. FMT from the D-gal-treated mice restored the intestinal structure (Fig. 5D) and increased the villus length compared to the ‘FMT-saline IR+’ group (Supplementary Fig. 2B). In addition, D-gal FMT significantly increased the expression levels of pro-epithelial genes compared to

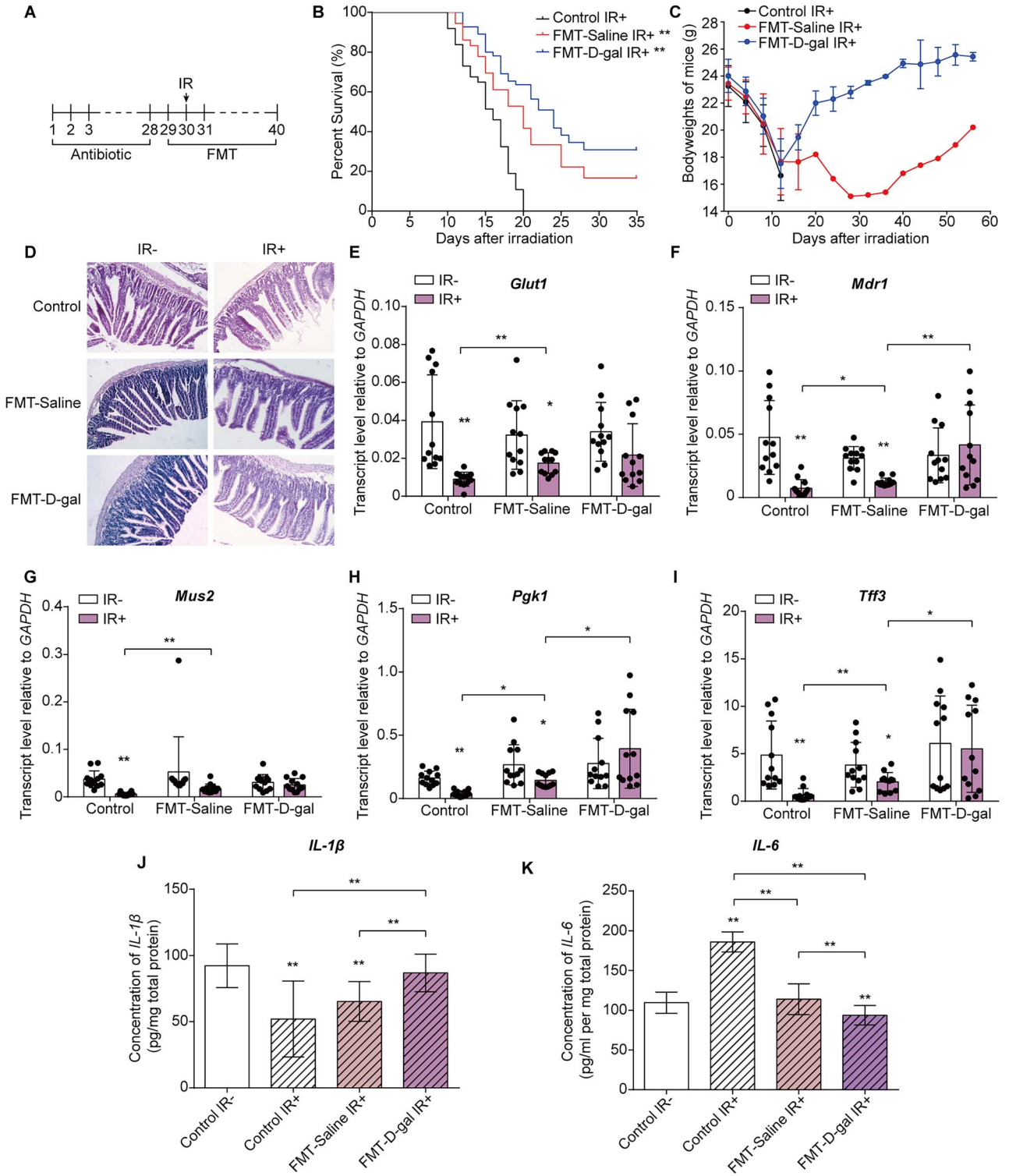


Fig. 5. FMT from D-gal-treated mice alleviated radiation-induced small intestine injury. (A) Schematic of the FMT assay. Mice were provided antibiotics in the drinking water for 4 weeks. Beginning on the day before irradiation, recipient mice were administered the microbiota mix from donor mice by oral gavage daily for 10 days. (B-C) Kaplan–Meier survival curve (B) and body weight (C) of mice in the FMT-saline and FMT-D-gal groups after the administration of 7.5 Gy of TBI; The number of mice

saline FMT or the non-irradiated controls (Fig. 5E–I). In addition, the IL-1 β and IL-6 level in the small intestine measured after TAI differed significantly between the saline and D-gal FMT groups and compared to the non-irradiated mice (Fig. 5J–K). Therefore, we hypothesized that the protective effects of D-gal on radiation-induced GI injury were attributed to changes in the predominant species of the gut microbiota.

D-gal altered the transcriptome of small intestine cells

D-gal-mediated O-GlcNAcylation of immunoglobulins and other glycoproteins is vital for immune cell activation, antigen presentation and antibody function [33, 34]. Therefore, we analyzed the expression levels of genes involved in galactose metabolism. As shown in Supplementary Fig. 5, D-gal did not significantly affect *Gale*, *Galc*, *Glb1*, *Galk1* and *Slc5a1* transcript levels in the intestines after irradiation as compared to ‘Saline IR+’ group. However, the transcript level of *B4galnt2* and *Slc35a2* increased significantly. Whole-transcriptome analysis of D-gal-treated human small intestine epithelial cells (HIEC-6) revealed two gene clusters (Fig. 6A–D). The first cluster consisting of 1073 genes did not change significantly after D-gal treatment and irradiation (Fig. 6B), and the KEGG (Kyoto Encyclopedia of Genes and Genomes) pathway analysis showed the enrichment of protein processing in the endoplasmic reticulum (ER) among these genes after D-gal treatment (Fig. 6C). The second cluster of 633 genes was significantly upregulated after D-gal treatment, regardless of irradiation (Fig. 6E), and was mainly enriched in pyrimidine metabolism, ribosome biogenesis and RNA transport (Fig. 6F). Taken together, D-gal may alter specific biological processes in the small intestines of irradiated mice. Since long-term D-gal injection may induce brain senescence, the protein level of the aging marker p16 was measured in the hippocampus of D-gal-injected mice using western blotting (Fig. 5SC). D-gal injection or irradiation failed to increase the p16 expression level, as indicated by the gray value (Fig. 5SD).

DISCUSSION

D-gal is crucial for the glycosylation of proteins in various biological processes. It accelerates senescence in aging models [35, 36] and induces oxidative damage in different organs, especially the nervous system. Therefore, D-gal is often used to mimic brain senescence in aging studies [37, 38]. However, a high dose of D-gal failed to induce senescence in the rat nervous system [39]. We found that 7.5 Gy of TBI and the administration of 750 mg/kg/day D-gal per day did not increase hippocampal levels of the senescence marker p16 (Supplementary Fig. 5C and D) in our murine study limited to male mice.

We believe that oral administration of D-gal would be the best clinical route of administration. But given our experimental results indicate that an oral dose of 500 mg/kg/day does not alter the post-irradiation survival of mice. Therefore, we did not use oral administration in subsequent work. D-gal protected against radiation-induced intestinal injury and improved the survival rate and body weight of mice when injected intraperitoneally. The transcriptome analysis further showed that D-gal affected intracellular signaling in small intestine cells. As compared to Saline treated mice, D-gal significantly changed transcript level of relative genes in absorption after irradiation (Supplementary Fig. 5B). Thus, D-gal might improve the efficiency of absorption in the small intestine after radiation injury at the transcript level. The transcriptome analysis and the expression level of genes in absorption indicates that D-gal not only influence the microorganisms in intestine of mice, but also by affecting some biological mechanisms in intestinal cells. Despite these encouraging therapeutic effects, 750 mg/kg/day is a high dose of D-gal, which is difficult to achieve in clinical situations.

D-gal significantly altered the gut microbiota composition, and FMT from D-gal-treated mice alleviated the effects of TAI, which is independent from the effect induced by D-gal on the transcriptome in intestinal cells, indicating that the gut microbiota is pivotal to the radio-protective effects of D-gal. Consistent with previous findings [15], radiation exposure significantly decreased the diversity of *Bacteroidetes* in the gut microbiota. In addition, the predominant class in the phylum *Firmicutes* shifted from *Clostridia* to *Bacilli* after irradiation. D-gal restored the abundance of *Bacteroidetes* but decreased its diversity. In addition, the predominant class of phylum *Firmicutes* in this group was *Erysipelotrichia*. On the other hand, the mice were treated with antibiotics in advance to avoid the effect of their own intestinal flora on the D-gal-treated flora in this work. Antibiotics also has an effect on the intestinal flora and other factors in the body of the mice. A disordered intestinal flora would also be detrimental to the repair of radiation damage in mice. Therefore, we performed 16 s analysis of intestinal flora before and after FMT to determine the success of flora colonization by FMT (Supplementary Fig. 4). However, such an approach is not the most rigorous for the study of intestinal flora. More rigorous flora colonization approaches are needed in future work to determine the effect of intestinal flora in the D-gal group.

Several intestinal microorganisms are crucial for intestinal immune barrier function, digestion and nutrient absorption, and some species protect against inflammation and radiation injury by producing specific metabolites [40]. For instance, *Erysipelotrichia* produces high levels of anti-inflammatory short-chain fatty acids (SCFAs) [41]. Gut dysbiosis often decreases SCFA levels and may lead to inflammatory bowel diseases [42]. SCFA enemas were used to treat radiation proctitis as early as the 1990s [43, 44]. Thus, the D-gal-induced elevation in

in each group are as followed: Control: $n = 37$; FMT-Saline IR+: $n = 36$, $P = 0.0015$; FMT-D-gal IR+: $n = 54$, $P < 0.0001$. (D) Representative images of HE-stained small intestine sections from the indicated groups. Small intestines were collected on the seventh day after the administration of 13 Gy of TAI. Tissues were collected from at least 6 mice in each group. (E–I) The transcript levels of *Glut1* (E), *Mdr1* (F), *Mus2* (G), *Pgk1* (H) and *Tff3* (I) in the small intestine of mice in different groups. The error bars in graphs means standard deviation of indicated data. * $P < 0.05$, ** $P < 0.01$; $n \geq 7$ mice per group. (J–K) IL-1 β and IL-6 levels in intestinal homogenates measured using ELISA. The error bars in graphs means standard deviation of indicated data. * $P < 0.05$, ** $P < 0.01$; $n \geq 7$ mice per group. Data in (E)–(K) were analyzed for differences using independent samples t-test. Stars without a horizontal line were generated by comparing the IR-group in indicated treatment (E–I) or ‘Control IR-’ group (J and K). Stars with a horizontal line mean that the two groups were compared.

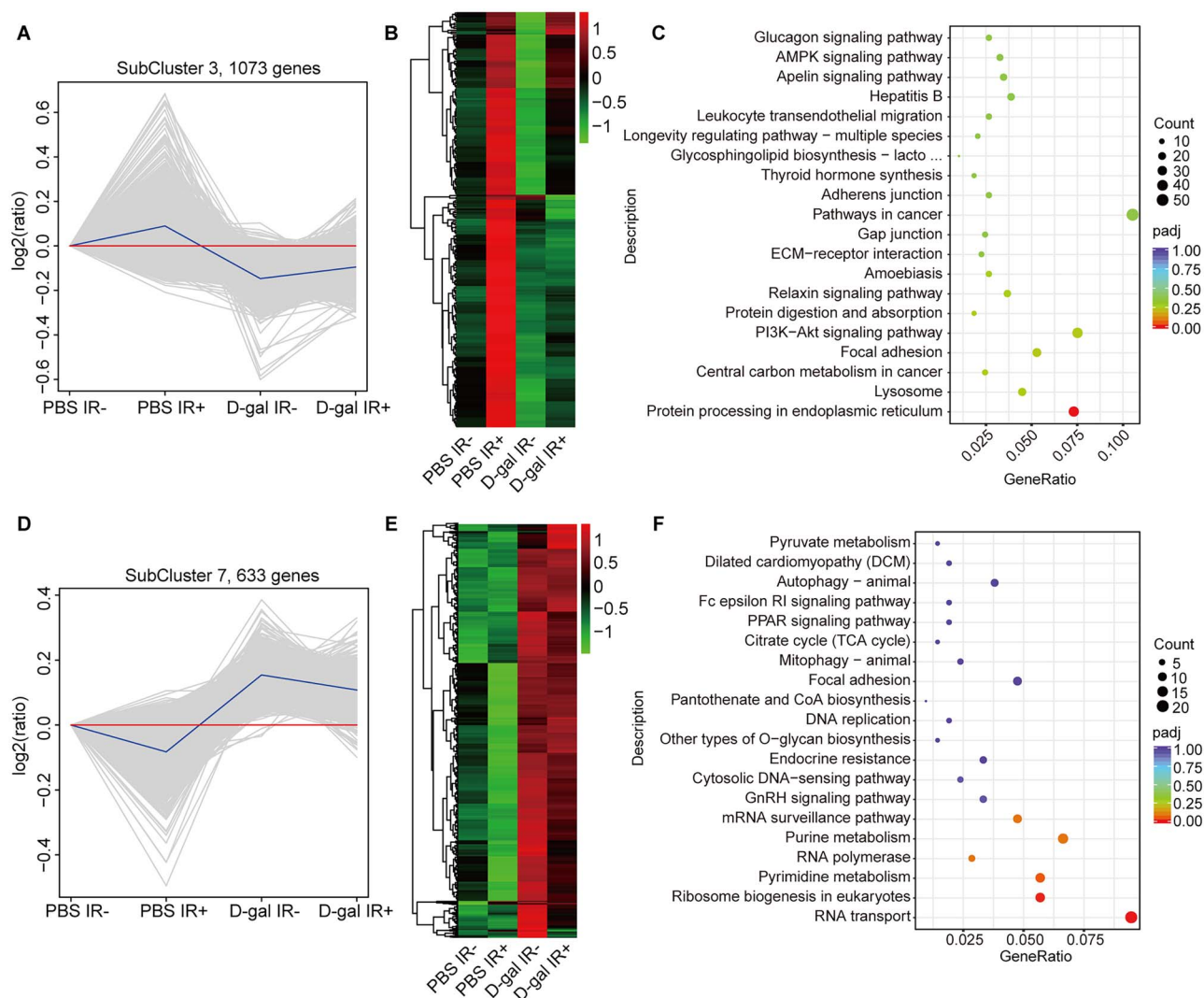


Fig. 6. D-gal altered the transcriptome of HIEC-6 cells. (A) Differentially expressed genes in subcluster 3 in the indicated groups. (B) Variations in the expression of 1073 genes identified in (A). (C) The Kyoto Encyclopedia of Genes and Genomes (KEGG) analysis of the genes shown in (A). (D) Differentially expressed genes in subcluster seven in the indicated groups. (E) Variations in the expression of the 663 genes identified in (D). (F) KEGG pathway enrichment analysis of the genes shown in (D).

Erysipelotrichia may increase the content of SCFAs and alleviate intestinal injury. However, we were unable to conclude that SCFA production is the primary mechanism underlying the radioprotective effect of D-gal since we did not measure SCFA levels. In addition, *Erysipelotrichia* produces multiple metabolites, and compounds other than SCFAs may also exert a therapeutic effect. D-gal also altered the transcriptome of cultured intestinal epithelial cells after irradiation, and the differentially expressed genes were enriched in the protein processing in ER, RNA transport and ribosome biogenesis pathways, which are associated with apoptosis. Gamma irradiation markedly increases intracellular ROS levels that lead to mitochondrial dysfunction [45] and excess Ca^{2+} influx [46], which disrupt ER-mitochondria signaling and eventually trigger the apoptotic cascade [47]. Therefore, D-gal may affect ER protein processing and the Ca^{2+} /ER/mitochondrial stress network following radiation injury.

D-gal protected against radiation-induced small intestine injury by altering the gut microbiota and increasing the abundance of the class *Erysipelotrichia*. Future studies should focus on the mechanisms underlying the radioprotective effects of D-gal and explore the metabolites of *Erysipelotrichia* with potential therapeutic effects on radiation injury. In addition, further longitudinal studies on D-gal may also identify novel therapeutic targets in radiation injury.

FUNDING

This work was supported by the Fundamental Research Funds for the Central Universities (grant number: 332019098), the National Natural Science Foundation of China (grant numbers: 81730086 and 81572969), CAMS Innovation Fund for Medical Sciences (grant numbers: 2018072-DZ-02, 2016-I2M-1-017 and 2016-I2M-B&R-13).

CONFLICT OF INTEREST

The authors declare no conflict of interest.

REFERENCES

- Bentzen SM. Preventing or reducing late side effects of radiation therapy: radiobiology meets molecular pathology. *Nat Rev Cancer* 2006;6:702–13.
- Kiang JG, Olabisi AO. Radiation: a poly-traumatic hit leading to multi-organ injury. *Cell Biosci* 2019;9:1–15.
- Fliedner TM, Graessle D, Meineke V et al. Pathophysiological principles underlying the blood cell concentration responses used to assess the severity of effect after accidental whole-body radiation exposure: an essential basis for an evidence-based clinical triage. *Exp Hematol* 2007;35:8–16.
- Abayomi OK. Pathogenesis of irradiation-induced cognitive dysfunction. *Acta oncologica (Stockholm, Sweden)* 1996;35:659–63.
- MacNaughton WK. Review article: new insights into the pathogenesis of radiation-induced intestinal dysfunction. *Aliment Pharmacol Ther* 2000;14:523–8.
- Dennis K, Zhang L, Lutz S et al. International patterns of practice in the management of radiation therapy-induced nausea and vomiting. *Int J Radiat Oncol Biol Phys* 2012;84:e49–60.
- Gwede CK. Overview of radiation- and chemoradiation-induced diarrhea. *Semin Oncol Nurs* 2003;19:6–10.
- Lu L, Jiang M, Zhu C et al. Amelioration of whole abdominal irradiation-induced intestinal injury in mice with 3,3'-Diindolylmethane (DIM). *Free Radic Biol Med* 2019;130:244–55.
- Fan S, Meng Q, Xu J et al. DIM (3,3'-diindolylmethane) confers protection against ionizing radiation by a unique mechanism. *Proc Natl Acad Sci U S A* 2013;110:18650–5.
- Fernandez-Gil B, Moneim AE, Ortiz F et al. Melatonin protects rats from radiotherapy-induced small intestine toxicity. *PLoS One* 2017;12:e0174474.
- Yamashita T, Kato T, Isogai T et al. Protective Effects of Taurine on the Radiation Exposure Induced Cellular Damages in the Mouse Intestine. *Adv Exp Med Biol* 2019;1155:443–50.
- Kumagai T, Rahman F, Smith AM. The microbiome and radiation induced-bowel injury: evidence for potential mechanistic role in disease pathogenesis. *Nutrients* 2018;10:1405.
- Rajilić-Stojanović M, Smidt H, de Vos WM. Diversity of the human gastrointestinal tract microbiota revisited. *Environ Microbiol* 2007;9:2125–36.
- Nam YD, Kim HJ, Seo JG et al. Impact of pelvic radiotherapy on gut microbiota of gynecological cancer patients revealed by massive pyrosequencing. *PLoS One* 2013;8:e82659.
- Hibberd AA, Lyra A, Ouwehand AC et al. Intestinal microbiota is altered in patients with colon cancer and modified by probiotic intervention. *BMJ Open Gastroenterol* 2017;4:e000145.
- Manichanh C, Varela E, Martinez C et al. The gut microbiota predispose to the pathophysiology of acute postradiotherapy diarrhea. *Am J Gastroenterol* 2008;103:1754–61.
- Wang A, Ling Z, Yang Z et al. Gut microbial dysbiosis may predict diarrhea and fatigue in patients undergoing pelvic cancer radiotherapy: a pilot study. *PLoS One* 2015;10:e0126312.
- Lee YS, Kim TY, Kim Y et al. Microbiota-derived lactate accelerates intestinal stem-cell-mediated epithelial development. *Cell Host Microbe* 2018;24:833–46.
- Ho SC, Liu JH, Wu RY. Establishment of the mimetic aging effect in mice caused by D-galactose. *Biogerontology* 2003;4:15–8.
- Shen YX, Xu SY, Wei W et al. Melatonin reduces memory changes and neural oxidative damage in mice treated with D-galactose. *J Pineal Res* 2002;32:173–8.
- Sun K, Yang P, Zhao R et al. Matrine attenuates D-galactose-induced aging-related behavior in mice via inhibition of cellular senescence and oxidative stress. *Oxidative Med Cell Longev* 2018;2018:7108604.
- Chen P, Chen F, Lei J et al. Activation of the miR-34a-Mediated SIRT1/mTOR signaling pathway by urolithin A attenuates D-galactose-induced brain aging in mice. *Neurotherapeutics* 2019;16:1269–82.
- Liang X, Yan Z, Ma W et al. Peroxiredoxin 4 protects against ovarian ageing by ameliorating D-galactose-induced oxidative damage in mice. *Cell Death Dis* 2020;11:1–10.
- Cui M, Xiao H, Li Y et al. Faecal microbiota transplantation protects against radiation-induced toxicity. 2017;9:448–61.
- Cui M, Xiao H, Li Y et al. Sexual dimorphism of gut microbiota dictates therapeutics efficacy of radiation injuries. *Advanced Science (Weinheim, Baden-Wuerttemberg, Germany)* 2019;6:1901048.
- Chen NY, Liu CW, Lin W et al. Extract of fructus cannabis ameliorates learning and memory impairment induced by D-galactose in an aging rats model. 2017;2017:4757520.
- Ahangarpour A, Oroojan AA. Exendin-4 protects mice from D-galactose-induced hepatic and pancreatic dysfunction. 2018;8:1418593.
- Qu Z, Zhang J, Yang H et al. Protective effect of tetrahydropalmatine against d-galactose induced memory impairment in rat. *Physiol Behav* 2016;154:114–25.
- Li W, Li N, Sui B et al. Anti-aging effect of fullerene on skin aging through derived stem cells in a mouse model. *Exp Ther Med* 2017;14:5045–50.
- Tang WH, Kitai T, Hazen SL. Gut Microbiota in Cardiovascular Health and Disease. *Circ Res* 2017;120:1183–96.
- Barcik W, Boutin RCT, Sokolowska M et al. The role of lung and gut microbiota in the pathology of asthma. *Immunity* 2020;52:241–55.
- Morais LH, HLT S. The gut microbiota-brain axis in behaviour and brain disorders. *Nat. Rev. Microbiol.* 2021;19:241–55.
- Shin H, Cha HJ, Na K et al. O-GlcNAcylation of the tumor suppressor FOXO3 triggers aberrant cancer cell growth. *Cancer Res* 2018;78:1214–24.
- Peng C, Zhu Y, Zhang W et al. Regulation of the Hippo-YAP pathway by glucose sensor O-GlcNAcylation. *Mol Cell* 2017;68:591–604.
- Fan SH, Zhang ZF, Zheng YL et al. Troxerutin protects the mouse kidney from d-galactose-caused injury through anti-inflammation and anti-oxidation. *Int Immunopharmacol* 2009;9:91–6.

36. Sun J, Zhang L, Zhang J et al. Protective effects of ginsenoside Rg1 on splenocytes and thymocytes in an aging rat model induced by d-galactose. *Int Immunopharmacol* 2018;58:94–102.
37. Wei H, Li L, Song Q et al. Behavioural study of the D-galactose induced aging model in C57BL/6J mice. *Behav Brain Res* 2005;157:245–51.
38. Li H, Zheng L, Chen C et al. Brain senescence caused by elevated levels of reactive metabolite methylglyoxal on D-galactose-induced aging mice. *Front Neurosci* 2019;13:1004.
39. Cardoso A, Magano S, Marrana F et al. D-galactose high-dose administration failed to induce accelerated aging changes in neurogenesis, anxiety, and spatial memory on young male wistar rats. *Rejuvenation Res* 2015;18:497–507.
40. Li Y, Dong J, Xiao H et al. Gut commensal derived-valeric acid protects against radiation injuries. *Gut microbes* 2020;11:789–806.
41. Schwartz A, Taras D, Schäfer K et al. Microbiota and SCFA in lean and overweight healthy subjects. *Obesity (Silver Spring, Md)* 2010;18:190–5.
42. Sun M, Wu W, Liu Z et al. Microbiota metabolite short chain fatty acids, GPCR, and inflammatory bowel diseases. *J Gastroenterol* 2017;52:1–8.
43. Al-Sabbagh R, Sinicrope FA, Sellin JH et al. Evaluation of short-chain fatty acid enemas: treatment of radiation proctitis. *Am J Gastroenterol* 1996;91:1814–6.
44. Talley NA, Chen F, King D et al. Short-chain fatty acids in the treatment of radiation proctitis: a randomized, double-blind, placebo-controlled, cross-over pilot trial. *Dis Colon Rectum* 1997;40:1046–50.
45. Yamamori T, Yasui H, Yamazumi M et al. Ionizing radiation induces mitochondrial reactive oxygen species production accompanied by upregulation of mitochondrial electron transport chain function and mitochondrial content under control of the cell cycle checkpoint. *Free Radic Biol Med* 2012;53:260–70.
46. Claro S, Oshiro ME, Mortara RA et al. γ -Rays-generated ROS induce apoptosis via mitochondrial and cell cycle alteration in smooth muscle cells. *Int J Radiat Biol* 2014;90:914–27.
47. Zheng P, Chen Q, Tian X et al. DNA damage triggers tubular endoplasmic reticulum extension to promote apoptosis by facilitating ER-mitochondria signaling. *Cell Res.* 2018;28:833–54.